Small Symmetrical Deformation of Thin Torus with Circular Cross-Section

Bohua Sun[1]

[1]*School of Civil Engineering & Institute of Mechanics and Technology, Xi'an University of Architecture and Technology, Xi'an 710055, China*

sunbohua@xauat.edu.cn

By introducing a variable transformation $\xi = \frac{1}{2}(\sin\theta + 1)$, a complex-form ordinary differential equation (ODE) for the small symmetrical deformation of an elastic torus is successfully transformed into the well-known Heun's ODE, whose exact solution is obtained in terms of Heun's functions. To overcome the computational difficulties of the complex-form ODE in dealing with boundary conditions, a real-form ODE system is proposed. A general code of numerical solution of the real-form ODE is written by using Maple. Some numerical studies are carried out and verified by both finite element analysis and H. Reissner's formulation. Our investigations show that both deformation and stress response of an elastic torus are sensitive to the radius ratio, and suggest that the analysis of a torus should be done by using the bending theory of a shell. A general Maple code is provided as essential part of this paper.

I. INTRODUCTION

The torus or toroidal shell, in full or partial geometric form, is widely used in structural engineering (Chang(Zhang) 1949 [1], Qian and Liang 1979 [2], Xia and Zhang 1986 [3], Zhang, Ren and Sun 1990 [4], Zhang and Zhang 1991 [5], 1994 [6], Audoly and Pomeau 2010 [7], Sun 2010 [8] 2012 [9], Clark 1950 [10, 11], Dahl 1953 [12], Novozhilov 1959 [13], Timoshenko and Woinowsky-Krieger 1959 [14], Flügge 1973 [15], Gol'denveizer 1961 [16] Sun 2013 [17], Föppl 1907 [18] Weihs 1911 [19], Wissler 1916 [20], Kuznetsov and Levyakov 2001 [21], Zingoni, Enoma and Govender 2015 [22], Jiammeepreecha and Chucheepsakul 2017 [23], Enoma and Zingoni 2020 [24], H. Reissner 1912 [25], Meissner 1915 [26], Tölke 1938 [27], E. Reissner 1949 [28], Tao 1959 [29], Steele 1965 [30], Sun 2018 [31]).

Among regular shells, such as circular cylindrical shells, conical shells, spherical shells, and tori, the deformation of the torus is one of the most difficulty topics due to its complicated topology.

The source of the difficulty comes from a geometric feature of the torus, whose Gauss curvature, $\kappa = \frac{\sin\theta}{a(R+a\sin\theta)}$, changes its sign as principal radius of curvature R_θ when the angle θ goes from 0 to 2π. This means that the Gauss curvature has a turning point, $\kappa = 0$ at $\theta = \pm\pi$. The geometry of the torus surface is elliptic in $\theta \in [0, \pi]$, parabolic at $\theta = 0$, and hyperbolic in $\theta \in [0, -\pi]$. Recall that the partial differential equations governing the elasticity of elliptic shells $\kappa > 0$ are themselves elliptic, while those for hyperbolic

shells $\kappa < 0$ are hyperbolic. This means that the equations for a toroidal shell are of a mixed type, i.e., elliptic in the outer half and hyperbolic in the inner half. The existence of a turning point in a complete torus is one source of difficulty in finding a solution. Owing to the difficulty of solving differential equations with both hyperbolic and elliptic regions (Chang(Zhang) 1949 [1], Qian and Liang 1979 [2], Xia and Zhang 1986 [3], Zhang, Ren and Sun 1990 [4], Zhang and Zhang 1991 [5], 1994 [6], Audoly and Pomeau 2010 [7], Sun 2010 [8] 2012 [9], Clark 1950 [10, 11], Dahl 1953 [12], Novozhilov 1959 [13], Timoshenko and Woinowsky-Krieger 1959 [14], Flügge 1973 [15], Gol'denveizer 1961 [16] Sun 2013 [17]), various proposed asymptotic solutions have singularity problem at the turning point (or called as crowns) of the Gauss curvature (Gol'denveizer 1961 [16]), where the Gauss curvature is zero (Chang(Zhang) 1949 [1], Qian and Liang 1979 [2], Xia and Zhang 1986 [3], Zhang, Ren and Sun 1990 [4], Zhang and Zhang 1991 [5], 1994 [6], Audoly and Pomeau 2010 [7], Sun 2010 [8] 2012 [9], Clark 1950 [10, 11], Dahl 1953 [12], Novozhilov 1959 [13], Wissler 1916 [20], Tölke 1938 [27], E. Reissner 1949 [28]).

The torus has been studied for more than 110 years ((Chang(Zhang) 1949 [1], Qian and Liang 1979 [2], Xia and Zhang 1986 [3], Zhang, Ren and Sun 1990 [4], Zhang and Zhang 1991 [5], 1994 [6], Audoly and Pomeau 2010 [7], Sun 2010 [8] 2012 [9], Clark 1950 [10, 11], Dahl 1953 [12], Novozhilov 1959 [13], Föppl 1907 [18] Weihs 1911 [19], Wissler 1916 [20], H. Reissner 1912 [25], Meissner 1915 [26], Tölke 1938 [27], E. Reissner 1949 [28], Tao 1959 [29], Steele 1965 [30], Sun 2018 [31]), and various aspects have been extensively investigated. In this paper, we will restrict ourselves to the small symmetrical deformation of elasic torus with a circular cross-section, and in particular with an emphasis on its theoretical formulation, associated analytical and numerical solutions. We will not touch topics such as non-circular cross-section, buckling, vibration, membrane solutions, and finite element analysis, which can be seen in the literature [21–24].

When the torus was first studied, high-order and complicated governing equations of a torus under symmetric loads were reduced to a single lower-order, complex-form ordinary differential equation (ODE) by Hans Reissner (1912)[25] when he was a professor at ETH in Switzerland. His colleague at ETH, Meissner (1915) [26], derived a complex-form equations for the shell of revolution. Hence, the first complex-form equation of the shells of revolution including torus is called the Reissner-Meissner equation. Reissner supervised a doctoral candidate, Gustav Weihs 1911 [19], who was the first person to receive a Dr.-Ing. in the field of torus research, in 1911. Unfortunately, I have not been able to find Weihs' thesis, and became familiar with his work from a citation by Wissler in his dissertation (Wissler 1916 [20]). Wissler was supervised by Meissner, and was the second person to receive a Dr.-Ing in the topic of torus. The first exact series solution of the complex-form equation was obtained by (Wissler 1916 [20]), but his work had no followers, perhaps because his series solution was not linked to any special functions and some computational

 doi:10.20944/preprints202012.0420.v3

challenge without computer.

In 1912, Hans Reissner took a professor position at TU Berlin and brought torus research there. Under Reissner's influence, his younger colleague, F. Tölke, made some simplifications and derived a simpler complex-form equation of torus (Tölke 1938 [27]). W. Chang (now spelling is W. Zhang), the current writer's post-doctoral supervisor at Tsinghua University during 1989-1991, was Tölke's doctoral Mitarbeiter, who proposed an asymptotic solution to Tölke's equation for a large radius ratio $\alpha = a/R$ of the torus. Zhang's solution was the first successful asymptotic solution valid for the large ratio in terms of Bessel functions (Chang(Zhang) 1949 [1]), and he received his Dr.-Ing. in 1944 from TU Berlin. In 1949, Hans Reissner's son Eric Resinner carried his father's legacy and researched the pure bending of curved tubes (E. Reissner 1949 [28]), and with his PhD syudent Clark, they published two papers (Clark 1950 [10, 11]) on the asymptotic solution and calculations. In 1953, Dahl studied toroidal-shell expansion joints (Dahl 1953 [12]). In 1959, Novozhilov published his celebrated monograph on the complex-form theory of shells, and gave an asymptotic solution to the symmetrical deformation of a torus (Novozhilov 1959 [13]). In 1959, Tao introduced a variable transformation and successfully transformed the Reissner-Meissner complex-form equation of a torus to a Heun-type ODE, and was the first person to find an exact solution that can be expressed in terms of Heun functions (Tao 1959 [29]). However, Tao did not perform any numerical calculations using his exact solution. Nevertheless, both Wissler and Tao reached the academic peak in the research of a torus with small deformation. In 1965, Steele investigated toroidal pressure vessels, and was able to make a concise comparison of the volume and weight properties of enough shapes to provide a convenient basis for their design (Steele 1965 [30]). Qian and Liang 1979 [2], Xia and Zhang 1986 [3], Zhang, Ren and Sun 1990 [4], Zhang and Zhang 1991 [5], 1994 [6] conducted further study, sought an enhanced asymptotic solution valid for the full domain of $\theta \in [0, 2\pi]$. Despite the complex-form formulation of all previous study, Sun was the first person to derive displacement-type equations of a torus and proposed a closed-form solution when the radius ratio tends to be null (Sun 2010 [8] 2012 [9]). The first monograph on torus was edited by Sun and published in 2012 (Sun 2012 [9]).

In 1959 Novozhilov systematically developed a comprehensive complex-form theory of thin shells and reformulated the symmetrical deformation of a torus (Novozhilov 1959 [13]), then he proposed an asymptotic solution for the thin torus. However, no exact solution in terms of special functions has been obtained for Novozhilov's complex-form ODE of symmetrical deformation of a torus. We will shoulder this burden and propose such a solution. Once we have the exact solution, the convergence over the full domain of $\theta \in [0, 2\pi]$ can then be guaranteed.

The remainder of this paper is organized as follows. Section 2 presents a formulation of the Novzhilov complex-form ordinary differential equation of a torus. Section 3 introduces a variable transformation and

Preprints (www.preprints.org) | NOT PEER-REVIEWED | Posted: 19 April 2021 doi:10.20944/preprints202012.0420.v3

finds an exact solution of the complex ODE. Section 4 splits the complex-ODE into a real-form ODE. In Section 5, we carry out numerical simulations for three cases by using our own Maple code. Section 6 discusses the difference between the membrane and bending theory of a torus. Section 7 h verifies our results by both finite element analysis and Hans Reissner's formulation. Section 8 provides conclusions and recommendations.

II. NOVOZHILOV'S FORMULATION OF SYMMETRICAL DEFORMATION OF ELASTIC TORUS

For the torus shown in Fig. 1, the positions of points on the middle surface will be determined by the angles θ and φ. Further, let R_1 be the radius of curvature of the meridian and R_2 the radius of curvature of the normal section, tangential to the parallel circle. This second radius is equal to the segment of the perpendicular to the middle surface between this surface and the axis of the torus.

The Lamé parameters in this case are determined by the expressions

$$A_1 = R_1 = a,\ A_2 = R_2 \sin\theta = R + a\sin\theta. \tag{1}$$

The principal radii of curvature are given by

$$R_1 = a,\ R_2 = R\frac{1+\alpha\sin\theta}{\sin\theta}, \tag{2}$$

where $\alpha = a/R$.

The complex-form governing equation of a torus for symmetrical deformation was obtained by Novozhilov (1959) [13] as follows:

$$(1+\alpha\sin\theta)\frac{d^2V}{d\theta^2} - \alpha\cos\theta\frac{dV}{d\theta} + 2id^2\sin\theta V = P(\theta), \tag{3}$$

where $V(\theta)$ is a auxiliary complex function of real variable θ and

$$P(\theta) = -2d^2(2d^2C + \frac{1}{2}i\alpha qa)\cos\theta, \tag{4}$$

$$2d^2 = \frac{a^2}{Rh}\sqrt{12(1-\nu^2)}, \tag{5}$$

where ν is the Poisson ratio, h is the thickness, q is the distributed load, and C is an integration constant that can be determined from static considerations. The analysis of the torus has thus been reduced to the problem of finding a solution for the ODE in (3).

Preprints (www.preprints.org) | NOT PEER-REVIEWED | Posted: 19 April 2021 doi:10.20944/preprints202012.0420.v3

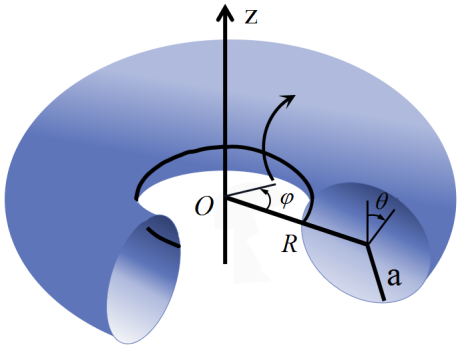

(a) Torus geometry

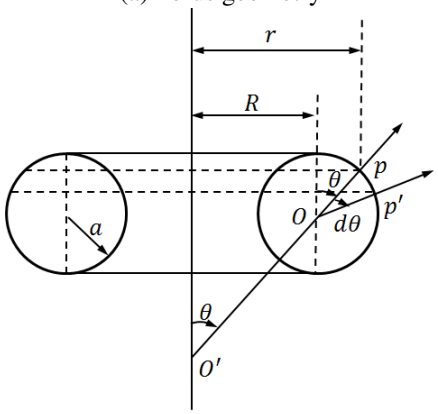

(b) Torus geometry cross-section

Figure 1: Torus geometry and cross-sectional. Principal radii of curvature are $R_1 = a$ and $R_2 = a + \frac{R}{\sin\theta}$; principal curvature $\kappa_1 = \frac{1}{a}$, $\kappa_2 = \frac{\sin\theta}{R+a\sin\theta}$; Gauss curvature $\kappa = \kappa_1\kappa_2 = \frac{\sin\theta}{a(R+a\sin\theta)}$.

Having the auxiliary function $V(\theta)$, all other quantities can be expressed in terms of $V(\theta)$. The resultant forces are

$$T_1 = -\frac{\alpha\cos\theta}{2d^2(1+\alpha\sin\theta)} Im(V) + \frac{qa}{2}\frac{2+\alpha\sin\theta}{1+\alpha\sin\theta} - \alpha C\frac{\alpha+\sin\theta}{(1+\alpha\sin\theta)^2}, \tag{6}$$

$$T_2 = -\frac{1}{2d^2} Im\left[\frac{d}{d\theta}\left(\frac{V}{1+\alpha\sin\theta}\right)\right] + \frac{qa}{2} + \alpha C\frac{\alpha+\sin\theta}{(1+\alpha\sin\theta)^2}, \tag{7}$$

where the Re and Im stand for the real and imaginary portion of the complex function $V(\theta)$. And resultant moments are

$$M_1 = -\frac{h}{2d^2\sqrt{12(1-\nu^2)}}\left\{\frac{\nu\alpha\cos\theta}{(1+\alpha\sin\theta)^2} Re(V) + Re\left[\frac{d}{d\theta}\left(\frac{V}{1+\alpha\sin\theta}\right)\right]\right\}, \tag{8}$$

$$M_2 = -\frac{h}{2d^2\sqrt{12(1-\nu^2)}}\left\{\frac{\alpha\cos\theta}{(1+\alpha\sin\theta)^2} Re(V) + \nu Re\left[\frac{d}{d\theta}\left(\frac{\nu V}{1+\alpha\sin\theta}\right)\right]\right\}, \tag{9}$$

Preprints (www.preprints.org) | NOT PEER-REVIEWED | Posted: 19 April 2021 doi:10.20944/preprints202012.0420.v3

resultant shear force is

$$N_1 = -\frac{h}{a\sqrt{12(1-\nu^2)}}\frac{\sin\theta Im(V) - 2d^2C\cos\theta}{(1+\alpha\sin\theta)^2}, \tag{10}$$

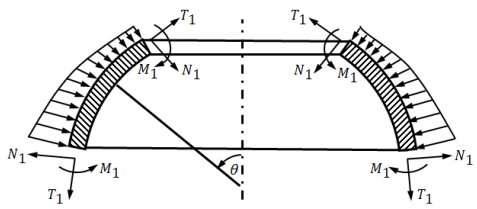

Figure 2: Components of forces and moments on middle surface

and angle of rotation of the tangent to the meridian is

$$\vartheta = -\frac{1}{Eh}\frac{1}{\alpha(1+\alpha\sin\theta)}Re(V). \tag{11}$$

The component of the displacement of an arbitrary point on the meridian in the direction of the axis of the torus is

$$\triangle_z = -a\int_0^\theta \vartheta\cos\theta d\theta + \triangle_z(0), \tag{12}$$

and the component of the displacement in the direction perpendicular to this axis is

$$\triangle_x = \frac{R}{Eh}(1+\alpha\sin\theta)(T_2 - \nu T_1). \tag{13}$$

The deformation displacement components of the middle surface in Fig. 3 can be obtained as

$$u = \triangle_x\cos\theta - \triangle_z\sin\theta, \tag{14}$$

$$w = \triangle_x\sin\theta + \triangle_z\cos\theta. \tag{15}$$

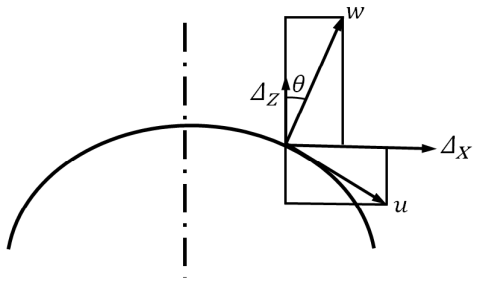

Figure 3: u and w are the components of displacement on the middle surface

Preprints (www.preprints.org) | NOT PEER-REVIEWED | Posted: 19 April 2021 doi:10.20944/preprints202012.0420.v3

The components of the middle surface forces are

$$Q_x = T_1 \cos\theta + N_1 \sin\theta, \tag{16}$$

$$Q_z = T_1 \sin\theta - N_1 \cos\theta, \tag{17}$$

where Q_z and Q_x, respectively, are the components of the forces in the direction of the axis of the torus and perpendicular to this axis, which act through the contemplated point of the meridian, as shown in Fig. 4.

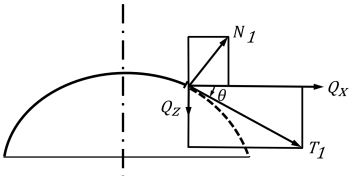

Figure 4: Q_z and Q_x are the components of the forces on the middle surface

III. EXACT SOLUTION OF SMALL SYMMETRICAL DEFORMATION OF TORUS

To solve Eq. 3, Wissler 1916 [20] introduced a variable transformation,

$$x = \sin\theta, \tag{18}$$

which leads to $dx = \cos\theta d\theta$, $\frac{dV}{d\theta} = \frac{dV}{dx}\frac{dx}{d\theta} = \cos\theta \frac{dV}{dx}$, and $\frac{d^2V}{d\theta^2} = \cos^2\theta \frac{d2V}{dx^2} - \sin\theta \frac{dV}{dx} = (1-x^2)\frac{d^2V}{dx2} - x\frac{dV}{dx}$. Hence Eq. 3 is transformed as follows:

$$(1-x^2)(1+\alpha x)\frac{d^2V}{dx^2} - (x+\alpha)\frac{dV}{dx} + 2id^2xV = P(x), \tag{19}$$

where $P(x) = -2d^2(2d^2C + \frac{1}{2}i\alpha qa)\sqrt{1-x^2}$.

Eq. 19 is a Fuchian-type differential equation whose series solution was given by Wissler 1916 [20], which is an exact solution but has not linked to any known functions.

To establish a relationship between Eq. 19 and well-known equations, let us introduce another variable transformation,

$$\xi = \frac{1}{2}x + \frac{1}{2} = \frac{1}{2}(\sin\theta + 1). \tag{20}$$

Thus $\frac{dV}{dx} = \frac{1}{2}\frac{dV}{d\xi}$, $\frac{d^2V}{dx^2} = \frac{1}{4}\frac{d^2V}{d\xi^2}$, and $1 - x^2 = -4\xi(\xi - 1)$, and Eq. 19 can be written as

Preprints (www.preprints.org) | NOT PEER-REVIEWED | Posted: 19 April 2021 doi:10.20944/preprints202012.0420.v3

$$\xi(\xi-1)[\xi-(\frac{1}{2}-\frac{1}{2\alpha})]\frac{d^2V}{d\xi^2}+\frac{1}{2\alpha}(\xi-\frac{1}{2}+\frac{\alpha}{2})\frac{dV}{d\xi}+(-\frac{4id^2}{\alpha}\xi+\frac{id^2}{\alpha})V=P(\xi), \tag{21}$$

where $P(\xi)=\frac{2d^2}{\alpha}(2d^2C+\frac{1}{2}i\alpha qa)\sqrt{\xi(1-\xi)}$; another common form is

$$\frac{d^2V}{d\xi^2}+(\frac{\frac{1}{2}}{\xi}+\frac{\frac{1}{2}}{\xi-1}+\frac{-1}{\xi-\frac{\alpha-1}{2\alpha}})\frac{dV}{d\xi}+\frac{-\frac{2id^2}{\alpha}\xi+\frac{id^2}{\alpha}}{\xi(\xi-1)(\xi-\frac{\alpha-1}{2\alpha})}V=f, \tag{22}$$

where

$$f=\frac{2d^2}{\alpha}\frac{1}{\xi(\xi-1)(\xi-\frac{\alpha-1}{2\alpha})}(2d^2C+\frac{1}{2}i\alpha aq). \tag{23}$$

It is easy to see that Eq. 21 or 22 is a Fuchian-type differential equation with four regular singular points: 0, 1, $\frac{\alpha-1}{2\alpha}$, and ∞. Eq. 22 was studied by Heun (1889)(Ronveaux 1995 [32], Marsden, Sirovich and Antman 1991 [34], and [33]), whose solutions can be represented by Heun's functions. Named after Karl Heun (1859–1929), these are unique local Frobenius solutions of a second-order linear ordinary differential equation of the Fuchsian type, which in the general case has four regular singular points.

The standard Heun ordinary differential equation is

$$\frac{d^2y(z)}{dz^2}+\frac{(\sigma+\beta+1)z^2+[(-\delta-\rho)c-\sigma+\delta-\beta-1]z+\rho c}{z(z-1)(z-c)}\frac{dy(z)}{dz}$$
$$+\frac{(z\beta\sigma-p)y(z)}{z(z-1)(z-c)}=0. \tag{24}$$

Its solution is given by

$$\begin{aligned}y(z)&=C_1HeunG(c,p,\beta,\sigma,\rho,\delta,z)\\&+C_2z^{1-\rho}HeunG(c,p-(-1+\rho)(\delta(-1+c)+\sigma+\beta-\rho+1),\\&\beta+1-\rho,\sigma-\rho+1,-\rho+2,\delta,z),\end{aligned} \tag{25}$$

where $HeunG(c,p,\beta,\sigma,\rho,\delta,z)$ is the Heun function, which can be expressed in series as

$$HeunG(c,p,\beta,\sigma,\rho,\delta,z)=1+\sigma\beta\sum_{n=1}^{\infty}\frac{G_n(p)}{n!(\rho)_n}(\frac{z}{c})^n, \tag{26}$$

where

$$\begin{aligned}n!&=n(n-1)...1,\quad (\rho)_n=\rho(\rho+1)(\rho+2)...(\rho+n-1),\\G_1(p)&=p,\quad G_2(p)=\sigma\beta p^2+[(\beta+\sigma-\delta+1)+(\rho+\delta)c]p-\beta\rho,\\G_{n+1}(p)&=\{n[(\sigma+\beta-\delta+n)+(\rho+\delta+n-1)c]+\sigma\beta p\}G_n(p)\\&-(c+n-1)(\beta+n-1)(\rho+n-1)ncG_{n-1}(p).\end{aligned} \tag{27}$$

Preprints (www.preprints.org) | NOT PEER-REVIEWED | Posted: 19 April 2021 doi:10.20944/preprints202012.0420.v3

Heun functions generalize the hypergeometric function. Because of their wide range of applications, they can be considered the 21st-century successors to hypergeometric functions (Ronveaux 1995 [32]).

The exact solution of Eq. 21 is the sum of a homogenous solution $V^h(x)$ and particular solution $V^p(x)$, i.e., $V = V^h + V^p$, both of which can be expressed by Heun functions. The homogenous solution can be given as

$$V^h(x) = C_1 y_1(x) + C_2 (x+1)^{\frac{1}{2}} y_2(x), \tag{28}$$

the solutions are

$$y_1(x) = HeunG(\frac{\alpha-1}{2\alpha}, -\frac{id^2}{\alpha}, a_1, a_2, \frac{1}{2}, \frac{1}{2}, \frac{1}{2}(x+1)), \tag{29}$$

$$y_2(x) = HeunG(\frac{\alpha-1}{2\alpha}, -\frac{1}{8}\frac{8id^2+3\alpha+1}{\alpha}, b_1, b_2, \frac{3}{2}, \frac{1}{2}, \frac{1}{2}(x+1)), \tag{30}$$

where

$$\begin{aligned} a_1 &= -\frac{1}{2}\frac{\sqrt{\alpha}\sqrt{8id^2+\alpha}+\alpha}{\alpha}, \\ a_2 &= \frac{1}{2}\frac{8id^2+\sqrt{\alpha}\sqrt{8id^2+\alpha}-\alpha}{\sqrt{\alpha}\sqrt{8id^2+\alpha}+2\alpha}, \\ b_1 &= -\frac{1}{2}\frac{\sqrt{8id^2+\alpha}}{\sqrt{\alpha}}, \\ b_2 &= \frac{1}{2}\frac{8id^2+2\sqrt{\alpha}\sqrt{8id^2+\alpha}+\alpha}{\sqrt{\alpha}\sqrt{8id^2+\alpha}+2\alpha}. \end{aligned} \tag{31}$$

Substituting Wissler's transformation $x = \sin\theta$ into the above solutions, we have

$$V^h(\theta) = C_1 y_1(\theta) + C_2 (\sin\theta+1)^{\frac{1}{2}} y_2(\theta), \tag{32}$$

where

$$y_1(\theta) = HeunG(\frac{\alpha-1}{2\alpha}, -\frac{id^2}{\alpha}, a_1, a_2, \frac{1}{2}, \frac{1}{2}, \frac{1}{2}(\sin\theta+1)), \tag{33}$$

$$y_2(\theta) = HeunG(\frac{\alpha-1}{2\alpha}, -\frac{1}{8}\frac{8id^2+3\alpha+1}{\alpha}, b_1, b_2, \frac{3}{2}, \frac{1}{2}, \frac{1}{2}(\sin\theta+1)). \tag{34}$$

A particular solution V^p in some simpler case can be expressed analytically by Heun functions, which will not be discussed here due to its complicated form. If the loading condition is not constant, then some integrations involving the Heun function in V^p may not be obtainable analytically, which unfortunately restricts the use of the exact solution.

Preprints (www.preprints.org) | NOT PEER-REVIEWED | Posted: 19 April 2021 doi:10.20944/preprints202012.0420.v3

IV. THE SPLIT OF THE NOVOZHILOV EQUATION

For further computation, the solution $V(\theta)$ must be split into real and imaginary parts, i.e., $Re(V)$ and $Im(V)$, respectively. However, this is not possible analytically due to the complicated expression of the Heun function. Without $Re(V)$ and $Im(V)$, no analytical components of force, moment, and displacement for the torus can be obtained, which limits the use of the complex-form analytical solution obtained in the previous section. Therefore, it is natural to seek a numerical solution based on the Novozhilov equation, i.e., Eq. 3.

Let us write $V(\theta)$ as

$$V(\theta) = A(\theta) + iB(\theta), \tag{35}$$

with the imaginary $i = \sqrt{-1}$, where $A(\theta) = Re(V)$ and $B(\theta) = Im(V)$ are the real and imaginary parts of $V(\theta)$. Substituting Eq. 35 in Eq. 3, we obtain

$$\begin{aligned}(1+\alpha\sin\theta)\frac{d^2A}{d\theta^2} - \alpha\cos\theta\frac{dA}{d\theta} - 2d^2\sin\theta B &= -2d^2(2d^2C)\cos\theta,\\ (1+\alpha\sin\theta)\frac{d^2B}{d\theta^2} - \alpha\cos\theta\frac{dB}{d\theta} + 2d^2\sin\theta A &= -2d^2(\frac{1}{2}\alpha qa)\cos\theta.\end{aligned} \tag{36}$$

Because we cannot analytically represent the integration of the displacement component of an arbitrary point on the meridian in the direction of the axis of a torus in Eq. 12, we use the corresponding differential equation,

$$\frac{d\triangle_z}{d\theta} - \frac{a}{Eh}\frac{A\cos\theta}{\alpha(1+\alpha\sin\theta)} = 0. \tag{37}$$

Now, the symmetrical deformation problem becomes one of finding the functions $A(\theta)$, $B(\theta)$, and $\triangle_z(\theta)$ in Eq.36 and 37..

With these functions, we can compute all other quantities, such as $T1$, T_2, M_1, M_2 and N_1, as well as u, w and ϑ. They can be expressed in terms of $A(\theta)$ and $B(\theta)$ as follows

$$T_1 = -\frac{\alpha\cos\theta}{2d^2(1+\alpha\sin\theta)}B(\theta) + \frac{qa}{2}\frac{2+\alpha\sin\theta}{1+\alpha\sin\theta} - \alpha C\frac{\alpha+\sin\theta}{(1+\alpha\sin\theta)^2}, \tag{38}$$

$$T_2 = -\frac{1}{2d^2}\left[\frac{d}{d\theta}(\frac{B(\theta)}{1+\alpha\sin\theta})\right] + \frac{qa}{2} + \alpha C\frac{\alpha+\sin\theta}{(1+\alpha\sin\theta)^2}. \tag{39}$$

Preprints (www.preprints.org) | NOT PEER-REVIEWED | Posted: 19 April 2021 doi:10.20944/preprints202012.0420.v3

The resultant moments are

$$M_1 = -\frac{h}{2d^2\sqrt{12(1-\nu^2)}}\left\{\frac{\nu\alpha\cos\theta}{(1+\alpha\sin\theta)^2}A(\theta) + \left[\frac{d}{d\theta}(\frac{A(\theta)}{1+\alpha\sin\theta})\right]\right\}, \tag{40}$$

$$M_2 = -\frac{h}{2d^2\sqrt{12(1-\nu^2)}}\left\{\frac{\alpha\cos\theta}{(1+\alpha\sin\theta)^2}A(\theta) + \nu\left[\frac{d}{d\theta}(\frac{A(\theta)}{1+\alpha\sin\theta})\right]\right\}, \tag{41}$$

the resultant shear force is

$$N_1 = -\frac{h}{a\sqrt{12(1-\nu^2)}}\frac{\sin\theta B(\theta) - 2d^2C\cos\theta}{(1+\alpha\sin\theta)^2}, \tag{42}$$

and the angle of rotation of the tangent to the meridian is

$$\vartheta = -\frac{1}{Eh}\frac{A(\theta)}{\alpha(1+\alpha\sin\theta)}. \tag{43}$$

The bending-related shell stresses are obtained by combining the direct stresses due to the stress resultants with the flexural stresses due to the bending moments,

$$\sigma_1 = \frac{T_1}{h} \pm \frac{6M_1}{h^2},\ \sigma_2 = \frac{T_2}{h} \pm \frac{6M_2}{h^2}. \tag{44}$$

The coupled differential equations (36) can be decoupled into differential equations about $A(\theta)$ and $B(\theta)$, both fourth-order ODEs, but no analytical solutions about $A(\theta)$ and $B(\theta)$ can be obtained.

V. NUMERICAL STUDIES OF SYMMETRICAL DEFORMATION OF TORUS

We numerically solve equations 36 and 37 for some typical cases. Unless otherwise stated, numerical calculations in this paper are based on the data in Table II.

We vary the radius $a = 0.18k$, $k = 1, 2, 3, 4, 5$, while other quantities are unchanged. Table I lists the geometric and material properties of the torus.

Table I: Data of torus

Quantities	R	a	h	E	ν	M_0	Q_0
Units	m	m	m	N/m^2	1	Nm	N
Data	1	$0.18k$	0.04	2.07×10^{11}	0.3	1	1

Note: Loads are set to unit values in all simulations. Since a small deformation is a linear problem, the superposition principle can be used with different loads, and solutions obtained by multiplying our results by an appropriate factor.

For simplification of picture presentation of our results, physical units will not be plotted in all drawings. For this purpose, we list all physical units of in Table II:

The geometry of these tori are shown in Fig. 5.

Preprints (www.preprints.org) | NOT PEER-REVIEWED | Posted: 19 April 2021 doi:10.20944/preprints202012.0420.v3

Table II: Physical units

R	a	h	E	ν	$M_1,\ M_2$	$T_1,\ T_2$	N_1	σ_1	ϑ	χ	u	w	Δ_z
m	m	m	N/m^2	1	N	N/m	N/m	N/m^2	1	1	m	m	m

Note: N is force physical unit and stands for Newton.

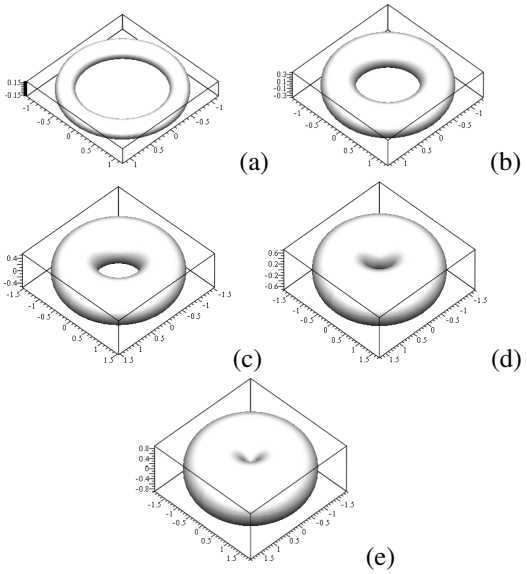

Figure 5: Torus geometry with different radii $a = 0.18k[m]$ $(k = 1, 2, 3, 4, 5)$

A. Complete torus with a penetrate cut along the parallel $\theta = \frac{\pi}{2}$ and loaded with vertical force Q_0

For a complete torus with a penetrate cut along the parallel $\theta = \frac{\pi}{2}$ and loaded with vertical force Q_0, the loading condition is shown in Fig. 6.

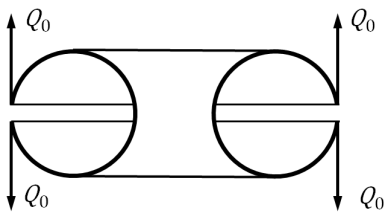

Figure 6: Torus with a cut along its parallel at $\theta = \frac{\pi}{2}$ or $\theta = -\frac{\pi}{2}$ under load Q_0

The boundary condition is:

$$\theta = \frac{\pi}{2} : T_1 = -\frac{Q_0}{2\pi(R+a)},\ N_1 = 0,\ M_1 = 0, \tag{45}$$

$$\theta = -\frac{3\pi}{2} : T_1 = -\frac{Q_0}{2\pi(R+a)},\ N_1 = 0,\ M_1 = 0,\ \Delta_z = 0. \tag{46}$$

Preprints (www.preprints.org) | NOT PEER-REVIEWED | Posted: 19 April 2021 doi:10.20944/preprints202012.0420.v3

For this problem, the constant C can be determined by the boundary condition of T_1 at $\theta = \frac{\pi}{2}$, namely

$$\theta = \frac{\pi}{2} : T_1 = -\frac{Q_0}{2\pi(R+a)}. \tag{47}$$

Taking into account the uniform distribution load $q = 0$, the above equation gives $C = \frac{1}{2\pi a}Q_0$. With the C, the boundary loading condition at both $\theta = \frac{\pi}{2}$ and $\theta = -\frac{3\pi}{2}$ are satisfied. The rest of the boundary condition can be expressed in terms of $A(\theta)$ and $B(\theta)$ as follows

$$\theta = \frac{\pi}{2} : B = 0, \ \frac{dA}{d\theta} = 0, \tag{48}$$

$$\theta = -\frac{3\pi}{2} : B = 0, \ \frac{dA}{d\theta} = 0, \ \Delta_z = 0. \tag{49}$$

Now, the problem becomes to solve $A(\theta)$ and $B(\theta)$ under conditions (48).

A general code for this case is written by Maple [35]. It is my honor to provide the code below, which can be used to solve your own torus problem by changing boundary conditions and some input data. The code is ready to run, you can just cut and pasted into Maple software. Enjoy your own computation with my Maple code. You are welcomed to contact me if you have any problem.

```
restart:with(plots): for k from 1 to 5 do: a:=0.18*k: R:=1: alpha:=a/(R): h:=0.04: mu:=0.3: E:=2.07e+11: q:=0:
Q:=1: C:=Q/(2*3.1415926*a): d:=sqrt(1/(2)*(sqrt(12*(1-mu*mu))*a*a)/(R*h)): kappa:=sqrt(12*(1-mu*mu)):
eta:=1+alpha*sin(theta):
equations:=eta*diff(A(theta),theta,theta)-(alpha*cos(theta))*diff(A(theta),theta)-2*d*d*sin(theta)          B(theta)=-
4*d*d*d*d*C*cos(theta),
eta*diff(B(theta),theta,theta)-(alpha*cos(theta))*diff(B(theta),theta)+2*d*d*sin(theta)                    A(theta)=-
2*d*d*((alpha*q*a)/(2)),
diff(Delta[z](theta),theta)=(a)/(E*h)*(A(theta))/(alpha*eta)*cos(theta);
boundary:=B(-(3* Pi)/(2))=0,B(Pi/(2))=0,D(A)(-(3*Pi)/(2))=0,D(A)(Pi/(2))=0,Delta[z](-(3*Pi)/(2))=0;
sol:=dsolve([equations,boundary],[A(theta),B(theta), Delta[z](theta)],numeric,
abserr=0.00001,output=listprocedure):
T1[k] := -alpha*cos(theta)*R*h*rhs(sol[4])/(eta*(a*a)*kappa)
+(1/2)*q*a*(2+alpha*sin(theta))/eta-alpha*C*(alpha+sin(theta))/(eta*eta);
T2[k] := -R*h*(rhs(sol[5])/eta+(diff(1/eta, theta))*rhs(sol[4]))/((a*a)*kappa)
+(1/2)*q*a+alpha*C*(alpha+sin(theta))/(eta*eta);
M1[k] := -(R*h*h)*(mu*alpha*cos(theta)*rhs(sol[2])/(eta*eta)
+rhs(sol[3])/eta+rhs(sol[2])*(diff(1/eta, theta)))/((a*a)*(kappa*kappa));
M2[k] := -(R*h*h)*(alpha*cos(theta)*rhs(sol[2])/(eta*eta)
+mu*rhs(sol[3])/eta+mu*rhs(sol[2])*(diff(1/eta, theta)))/((a*a)*kappa*kappa);
N1[k] := -h*sin(theta)*rhs(sol[4])/(a*kappa*(eta*eta))+a*C*cos(theta)/(R*(eta*eta));
z[k] := rhs(sol[6]):
```

Preprints (www.preprints.org) | NOT PEER-REVIEWED | Posted: 19 April 2021 doi:10.20944/preprints202012.0420.v3


```
od;
plot([seq(M1[k](theta), k = 1 .. 5)], theta = -3*Pi*(1/2) .. (1/2)*Pi,
legend = [”k=1”, ”k=2”, ”k=3”, ”k=4”, ”k=5”], linestyle = [1, 3, 2, 4, 5],
color = [”black”, ”red”, ”blue”, ”orange”, ”navy”], axes = boxed);
plot([seq(M2[k](theta), k = 1 .. 5)], theta = -3*Pi*(1/2) .. (1/2)*Pi,
legend = [”k=1”, ”k=2”, ”k=3”, ”k=4”, ”k=5”], linestyle = [1, 3, 2, 4, 5],
color = [”black”, ”red”, ”blue”, ”orange”, ”navy”], axes = boxed);
plot([seq(T1[k](theta), k = 1 .. 5)], theta = -3*Pi*(1/2) .. (1/2)*Pi,
legend = [”k=1”, ”k=2”, ”k=3”, ”k=4”, ”k=5”], linestyle = [1, 3, 2, 4, 5],
color = [”black”, ”red”, ”blue”, ”orange”, ”navy”], axes = boxed);
plot([seq(T2[k](theta), k = 1 .. 5)], theta = -3*Pi*(1/2) .. (1/2)*Pi,
legend = [”k=1”, ”k=2”, ”k=3”, ”k=4”, ”k=5”], linestyle = [1, 3, 2, 4, 5],
color = [”black”, ”red”, ”blue”, ”orange”, ”navy”], axes = boxed);
plot([seq(N1[k](theta), k = 1 .. 5)], theta = -3*Pi*(1/2) .. (1/2)*Pi,
legend = [”k=1”, ”k=2”, ”k=3”, ”k=4”, ”k=5”], linestyle = [1, 3, 2, 4, 5],
color = [”black”, ”red”, ”blue”, ”orange”, ”navy”], axes = boxed);
plot([seq(z[k](theta), k = 1 .. 5)], theta = -3*Pi*(1/2) .. (1/2)*Pi,
legend = [”k=1”, ”k=2”, ”k=3”, ”k=4”, ”k=5”], linestyle = [1, 3, 2, 4, 5],
color = [”black”, ”red”, ”blue”, ”orange”, ”navy”], axes = boxed);
```

With the help of the above Maple code, some numerical results have been obtained and are shown in Fig. 7, 8, 9, and Fig. 10.

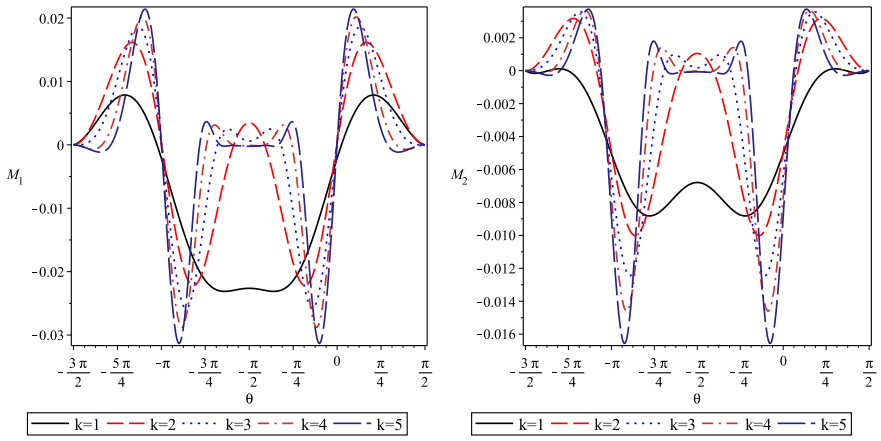

Figure 7: Bending moments for different radius $a = 0.18k[m]$. Left: Bending moment M_1 for torus with $a = 0.36$, and $M_1(\pi/4) = 0.01319738724[Nm]$; Right: Bending moment M_2 for torus with $a = 0.36$, and $M_2(\pi/4) = 0.003058118422[Nm]$.

The above all figures indicate that all quantities such as bending moments, surface forces, shear force, and displacement are strongly effected by the radius ratio $\alpha = a/R$, and vary dramatically with θ both near

Preprints (www.preprints.org) | NOT PEER-REVIEWED | Posted: 19 April 2021 doi:10.20944/preprints202012.0420.v3

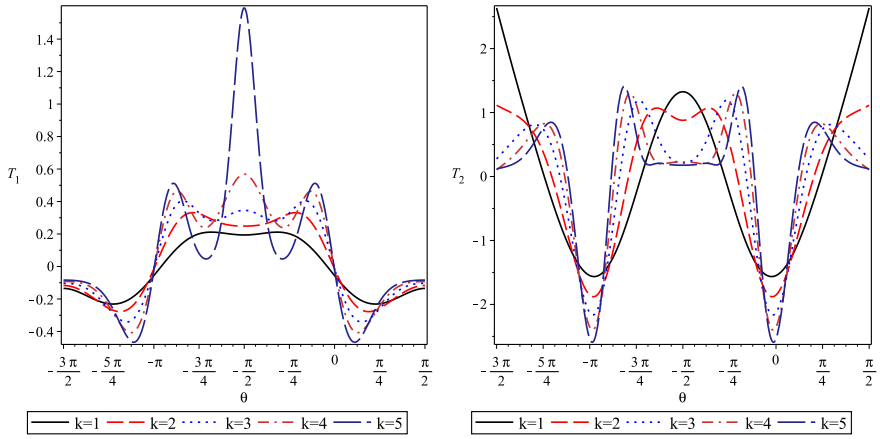

Figure 8: Membranae force for different radius $a = 0.18k[m]$. Left: Membranae force T_1; Right: Membranae force T_2.

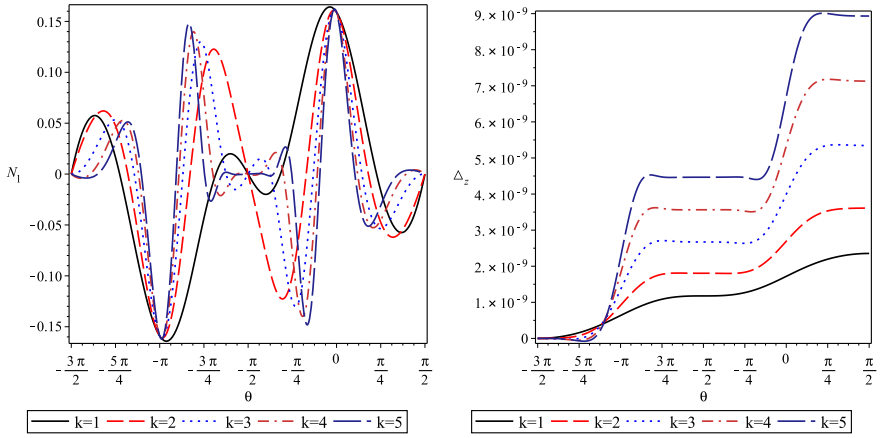

Figure 9: Shear force for different radius $a = 0.18k[m]$. Left: Shear force N_1; Right: relative displacement in z direction Δ_z.

to and far from the edge.

B. Complete torus with penetrate cut along the parallel $\theta = \frac{\pi}{2}$ and loaded with bending moment M_0

Fig. 11 shows a complete torus with a penetrate cut along the parallel $\theta = \frac{\pi}{2}$ and loaded with distributed bending moment M_0.

The boundary condition is:

Preprints (www.preprints.org) | NOT PEER-REVIEWED | Posted: 19 April 2021 doi:10.20944/preprints202012.0420.v3

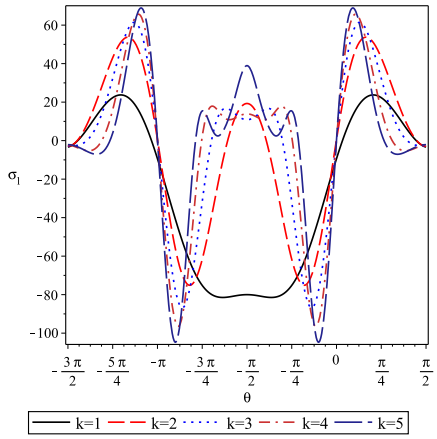

Figure 10: Stress σ_1 for different radius $a = 0.18k[m]$.

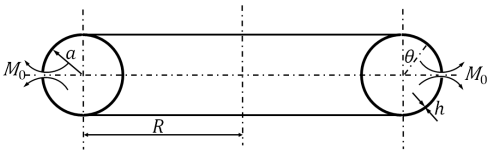

Figure 11: Torus with a cut along its parallel at $\theta = \frac{\pi}{2}$ or $\theta = -\frac{\pi}{2}$ under a pure moment M_0

$$\theta = \frac{\pi}{2} : T_1 = 0,\ N_1 = 0,\ M_1 = -\frac{M_0}{2\pi(R+a)}, \tag{50}$$

$$\theta = -\frac{3\pi}{2} : T_1 = 0,\ N_1 = 0,\ M_1 = -\frac{M_0}{2\pi(R+a)},\ \Delta_z = 0. \tag{51}$$

For this problem, the constant C can be determined by the boundary condition of T_1 at $\theta = \frac{\pi}{2}$, namely

$$\theta = -\frac{\pi}{2} :\ T_1 = 0. \tag{52}$$

Taking into account the uniform distribution load $q = 0$, the above equation gives $C = 0$, and the boundary loading condition at both $\theta = \frac{\pi}{2}$ and $\theta = -\frac{3\pi}{2}$ are satisfied. The rest of the boundary condition can be expressed in terms of functions $A(\theta)$ and $B(\theta)$, as follows:

$$\theta = \frac{\pi}{2} : B = 0,\ \frac{dA}{d\theta} = -\frac{6(\nu^2-1)a^2}{\pi R^2 h^2} M_0, \tag{53}$$

$$\theta = -\frac{3\pi}{2} : B = 0,\ \frac{dA}{d\theta} = -\frac{6(\nu^2-1)a^2}{\pi R^2 h^2} M_0,\ \Delta_z = 0. \tag{54}$$

The problem now becomes to find $A(\theta)$ and $B(\theta)$ under conditions (53). The numerical results are shown in Fig. 12, 13, and 14, which indicate that all quantities such as the bending moments, surface forces,

Preprints (www.preprints.org) | NOT PEER-REVIEWED | Posted: 19 April 2021 doi:10.20944/preprints202012.0420.v3

shear force, and displacement are strongly affected by the radius ratio $\alpha = a/R$, and vary dramatically with the angle θ both near to and far from the edge.

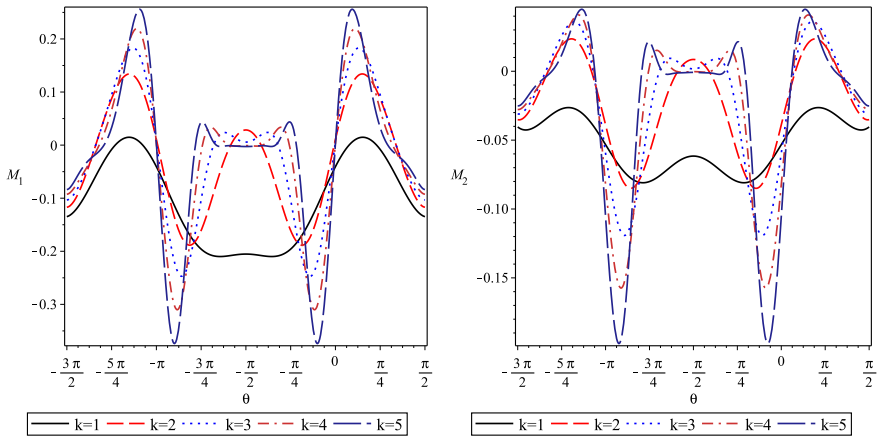

Figure 12: Bending moments for different radius $a = 0.18k[m]$. Left: Bending moment M_1; Right: Bending moment M_2.

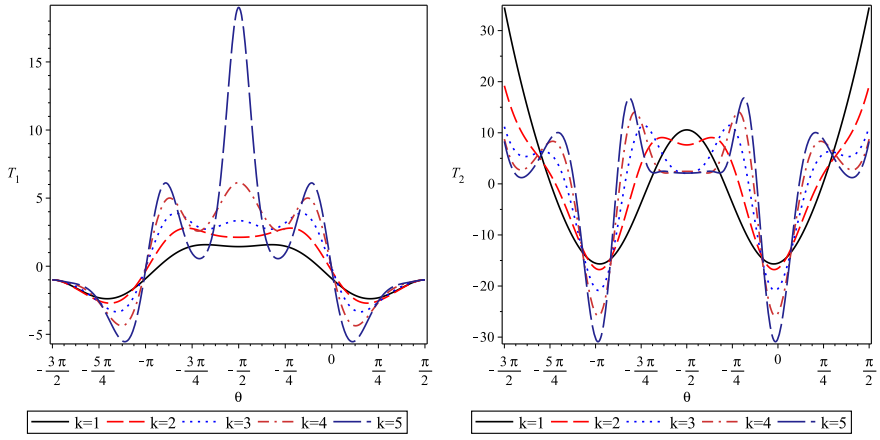

Figure 13: Membranae force for different radius $a = 0.18k[m]$. Left: Membranae force T_1; Right: Membranae force T_2.

C. Half torus under edge vertical force along its parallel at $\theta = \frac{\pi}{2}$

If we remove the inner region of a torus, we will have a half torus consisting of the outer region. The half torus is under a vertical load along its parallel at $\theta = \frac{\pi}{2}$ and $\theta = \pi$, as shown in Fig. 15.

Taking into account of symmetric nature, we only consider the top half. Thus we have boundary condition:

Preprints (www.preprints.org) | NOT PEER-REVIEWED | Posted: 19 April 2021 doi:10.20944/preprints202012.0420.v3

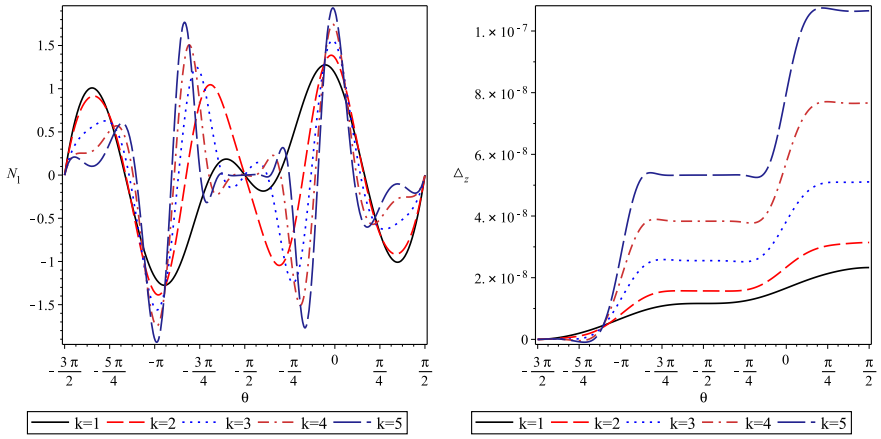

Figure 14: Shear force for different radius $a = 0.18k[m]$. Left: Shear force N_1; Right: relative displacement in z direction Δ_z.

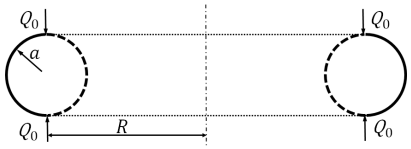

Figure 15: Torus with a cut along its parallel at $\theta = \frac{\pi}{2}$ or $\theta = -\frac{\pi}{2}$ under a force Q_0

$$\theta = 0 : T_1 = 0,\ M_1 = 0,\ N_1 = -\frac{Q_0}{2\pi R}, \tag{55}$$

$$\theta = \frac{\pi}{2} : N_1 = 0,\ \vartheta = 0,\ \Delta_z = 0. \tag{56}$$

For this problem, the constant C can be determined by the boundary condition of N_1 at $\theta = 0$, namely

$$\theta = 0 :\ N_1 = -\frac{Q_0}{2\pi R}. \tag{57}$$

We obtain $C = -\frac{Q_0}{2\pi a}$, in which case the boundary loading condition at both $\theta = 0$ and $\theta = \pi$ are satisfied.

The boundary condition in 55 can be expressed in terms of $A(\theta)$ and $B(\theta)$, as follows:

$$\theta = 0 : Rh\pi B - \alpha a Q_0\sqrt{3(1-\nu^2)} = 0,\ (\nu - 1)A + \frac{dA}{d\theta} = 0, \tag{58}$$

$$\theta = \pi/2 : A = 0,\ B = 0,\ \Delta_z = 0. \tag{59}$$

The problem now becomes to solve $A(\theta)$ and $B(\theta)$ under conditions (58) and (59). The numerical results are shown in Fig. 16, 17, and 18, and the stress is shown in Fig. 19.

Preprints (www.preprints.org) | NOT PEER-REVIEWED | Posted: 19 April 2021 doi:10.20944/preprints202012.0420.v3

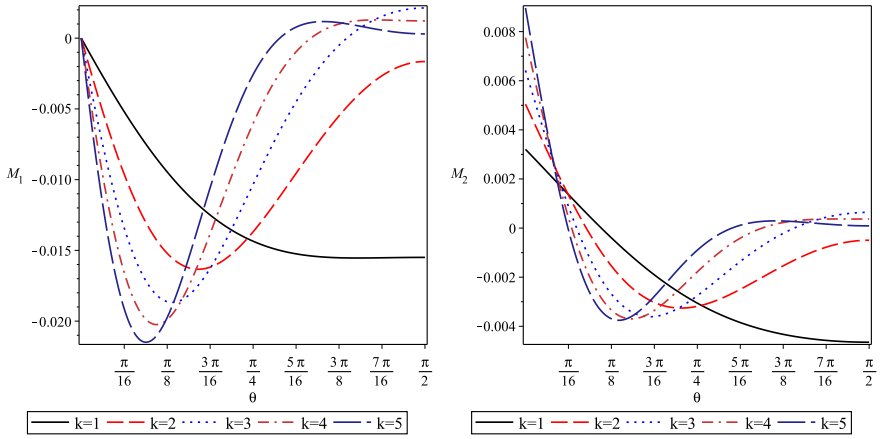

Figure 16: Bending moments for different radius $a = 0.18k[m]$. Left: Bending moment M_1; Right: Bending moment M_2.

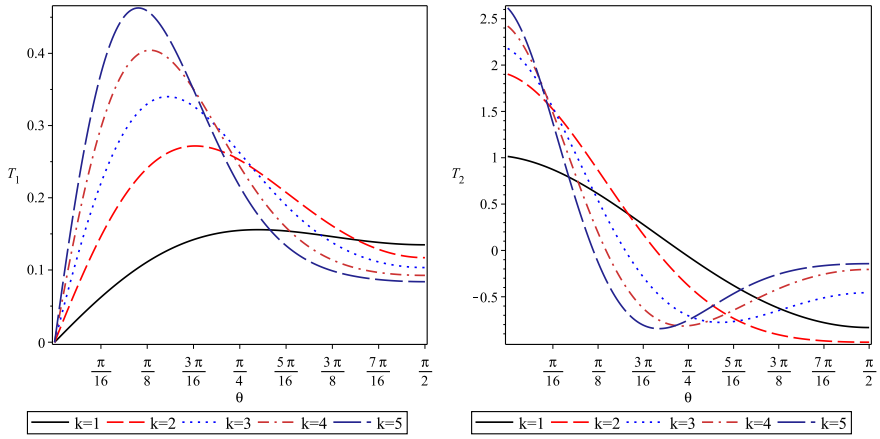

Figure 17: Membranae force for different radius $a = 0.18k[m]$. Left: Membranae force T_1; Right: Membranae force T_2.

These figures indicate that all quantities, such as bending moments, membranae forces, shear force, and displacement, are strongly affected by the radius ratio $\alpha = a/R$, and vary dramatically with θ both near to and far from the edge.

VI. COMPARISON BETWEEN THE MEMBRANE THEORY AND BENDING THEORY OF TORUS

In the history of theory of shells, a membrane theory is developed to simplify the analysis of shell structures. In the study of the equilibrium of the shell element, this theory neglects all bending moments, which means that only surface forces T_1, T_2 are left. The membrane theory can make valuable predictions for shells with very small bending stiffness or when the changes of curvature and twist of the middle surface

Preprints (www.preprints.org) | NOT PEER-REVIEWED | Posted: 19 April 2021 doi:10.20944/preprints202012.0420.v3

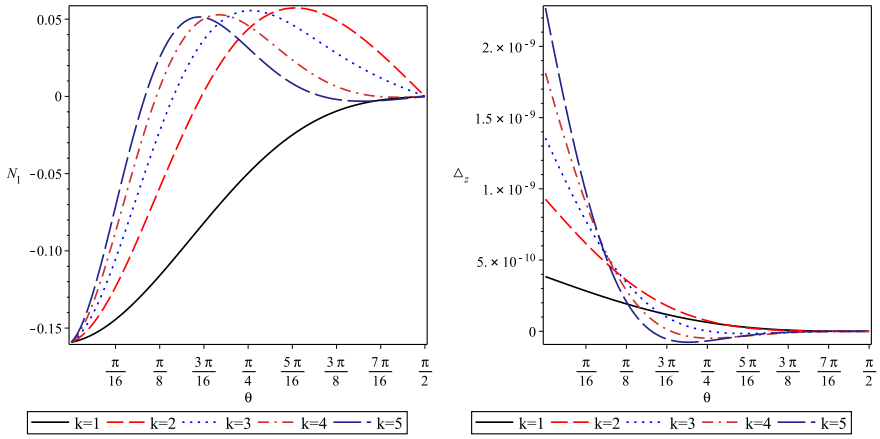

Figure 18: Shear force for different radius $a = 0.18k[m]$. Left: Shear force N_1; Right: relative displacement in z direction Δ_z.

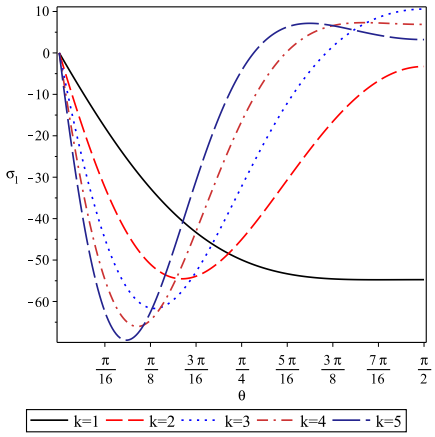

Figure 19: Stress σ_1 for different radius $a = 0.18k[m]$.

are very small. The above case studies show that membrane theory cannot provide reasonable results for a torus due to the strong variation of its curvature.

To obtain a clear picture of the difference between a membrane and the theory of a torus, let us perform comparisons for the above three case studies. For the case study in Section 5.1, the surface force is shown in Fig. 20.

For the case study in Section 5.2, the comparison is shown in Fig. 21.

For the case study in Section 5.3, the comparison is shown in Fig. 22.

Fig. 20, 21, and 22 show that the results obtained from bending theory and membrane theory are totally different except at boundaries.

These comparison studies reveal that the results from the membrane theory of the torus are questionable. Therefore, the bending theory of shells should be used for the analysis of a torus.

Preprints (www.preprints.org) | NOT PEER-REVIEWED | Posted: 19 April 2021 doi:10.20944/preprints202012.0420.v3

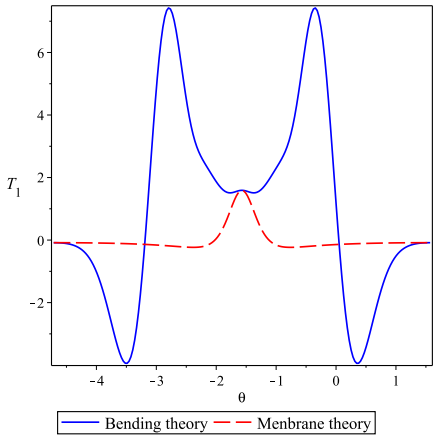

Figure 20: Membranae force T_1 for torus radius $a = 0.36[m]$.

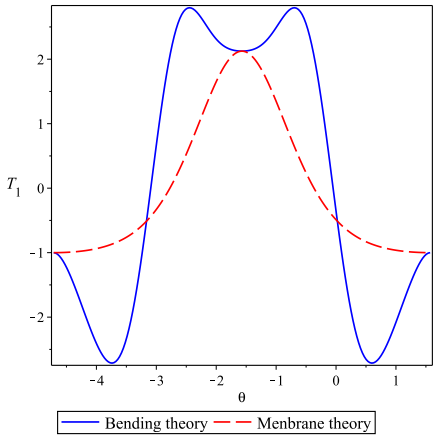

Figure 21: Membranae force T_1 for torus radius $a = 0.36[m]$.

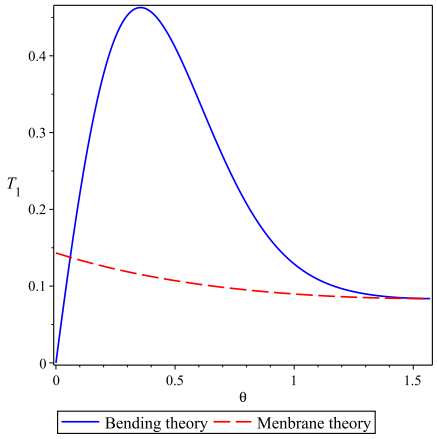

Figure 22: Membranae force T_1 for torus radius $a = 0.36[m]$.

Preprints (www.preprints.org) | NOT PEER-REVIEWED | Posted: 19 April 2021 doi:10.20944/preprints202012.0420.v3

VII. RESULTS VALIDATION

A. Verification of our results by finite element analysis

To verify our result, we carried out a finite element analysis for the case study in Section 5.1. The comparisons are shown in Fig. 23.

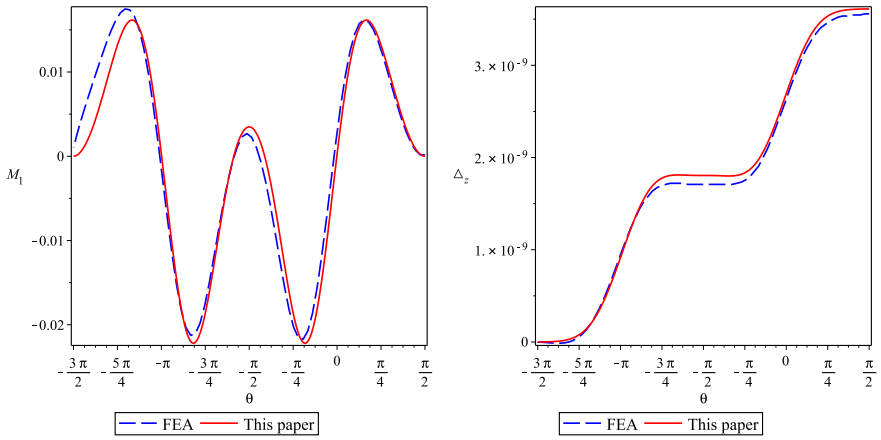

Figure 23: Results for torus radius with $a = 0.36[m]$ in Section 5.1, as shown in Fig. 6. Left: Bending moment M_1; Right: Vertical displacement Δ_z, this paper gives $\Delta_z(\pi/2) = 3.61080495828841 \times 10^{-9}[m]$, FEM gives $\Delta_z(\pi/2) = 3.557581142 \times 10^{-9}[m]$.

The finite element results were simulated by ABAQUS with shell element S4R. We applied the boundary condition $\triangle_z(-3\pi/2) = 0$ to cancel the rigid body motion, which might be the reason for minor differences in the range $\theta \in [-3\pi/2, -5\pi/4]$. From physics point of view, our result is symmetric respect to the axes of $\theta = -\pi/2$ while the FEA has slightly symmetry breaking. Therefore, our results are more trustable since the finite element analysis supports our numerical prediction nicely.

B. Comparison with Hans Reisnner's formulation of torus

In the theory of shells of revolution under axisymmetric load, according to Timoshenko and Woinowsky-Krieger 1959 [14], the decisive step was the introduction of N_1 and χ as unknowns by H. Reissner 1912 [25]. The idea has been much extended by E. Meissner 1925 [26]. The formulation of Reissner-Meissner of shells of revaluation with constant thickness can be found in the masterpieces of Flügge 1973 [15] and presented as follows:

Preprints (www.preprints.org) | NOT PEER-REVIEWED | Posted: 19 April 2021 doi:10.20944/preprints202012.0420.v3

$$\frac{R_2}{R_1}\frac{d^2\chi}{d\theta^2}+[\frac{R_2}{R_1}\cot\theta+\frac{d}{d\theta}(\frac{R_2}{R_1})]\frac{d\chi}{d\theta}-(\frac{R_1}{R_2}\cot^2\theta+\nu)\chi=\frac{1}{B}R_1R_2N_1, \tag{60}$$

$$\frac{R_2}{R_1}\frac{d^2}{d\theta^2}(R_2N_1)+[\frac{R_2}{R_1}\cot\theta+\frac{d}{d\theta}(\frac{R_2}{R_1})]\frac{d}{d\theta}(R_2N_1)-(\frac{R_1}{R_2}\cot^2\theta-\nu)(R_2N_1)$$
$$=-B(1-\nu^2)R_1\chi+Pg(\theta), \tag{61}$$

where χ is the angle by which an element $rd\theta$ of the meridian rotates during deformation, $r=R_2\sin\theta$, the load term P is constant to be determined by the value of $T_1(\pi/2)=-\frac{P}{2\pi R_2}$ and

$$g(\theta)=\frac{1}{2\pi\sin^2\theta}[\frac{R_1^2-R_2^2}{R_1R_2}\cot\theta+\frac{d}{d\theta}(\frac{R_2}{R_1})]. \tag{62}$$

The resultant membranae forces can be represented by shear force N_1:

$$T_1=-N_1\cot\theta-\frac{P}{2\pi R_2}\frac{1}{\sin^2\theta}, \tag{63}$$

$$T_2=-\frac{1}{R_1}\frac{d}{d\theta}(R_2N_1)+\frac{P}{2\pi R_1}\frac{1}{\sin^2\theta}, \tag{64}$$

Substituting the principal radii, ie., R_1, R_2 into Eq.60 will give governing equation for torus as follows:

$$\frac{R+a\sin\theta}{a\sin\theta}\frac{d^2\chi}{d\theta^2}+[\frac{R+a\sin\theta}{a\sin\theta}\cot\theta+\frac{d}{d\theta}(\frac{R+a\sin\theta}{a\sin\theta})]\frac{d\chi}{d\theta}$$
$$-(\frac{a\sin\theta}{R+a\sin\theta}\cot^2\theta+\nu)\chi=\frac{1}{B}a(a+\frac{R}{\sin\theta})N_1, \tag{65}$$

$$[\frac{R+a\sin\theta}{a\sin\theta}\cot\theta+\frac{d}{d\theta}(\frac{R+a\sin\theta}{a\sin\theta})]\frac{d}{d\theta}[(a+\frac{R}{\sin\theta})N_1]$$
$$\frac{R+a\sin\theta}{a\sin\theta}\frac{d^2}{d\theta^2}[(a+\frac{R}{\sin\theta})N_1]-(\frac{a\sin\theta}{R+a\sin\theta}\cot^2\theta-\nu)(a+\frac{R}{\sin\theta})N_1$$
$$=-B(1-\nu^2)a\chi+Pg(\theta). \tag{66}$$

Once we obtain the shear force N_1 and rotation χ, one can compute all other quantities, such as $T1$, T_2, M_1, M_2, as well as u, w.

The problem of elastic torus becomes to find the shear force N_1 and rotation χ from Eq.65 and 66. Obviously, Eq.65 and 66 are complicated and hard to be solved analytically.

To verify our numerical results obtained from Novozhilov's formulation, we write a Maple code to compute the Eq.65 and 66 numerically. Detailed Reissner's formulation, Maple coding and numerical simulations will be presented in another paper. The data of torus is given in Table II.

The numerical simulation here show that the results of two formulations proposed by Novozhilov and Hans Reissner are agree each other very well, which provides a good supportive evidence about the correctness of our simulation.

Preprints (www.preprints.org) | NOT PEER-REVIEWED | Posted: 19 April 2021 doi:10.20944/preprints202012.0420.v3

Table III: Data of torus [24]

Quantities	R	a	h	E	ν	Q_0
Units	m	m	m	N/m^2	1	N
Data	30	10	0.05	2.0×10^{11}	0.3	1

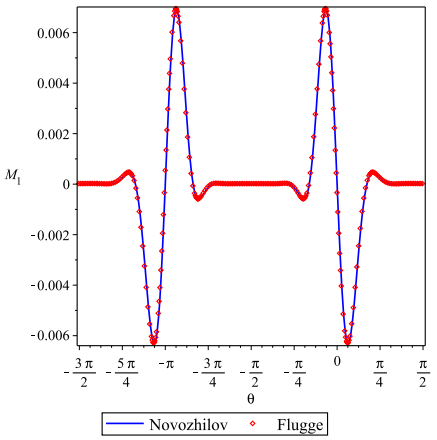

Figure 24: Bending moments M_1 for problem as shown in Fig. 6.

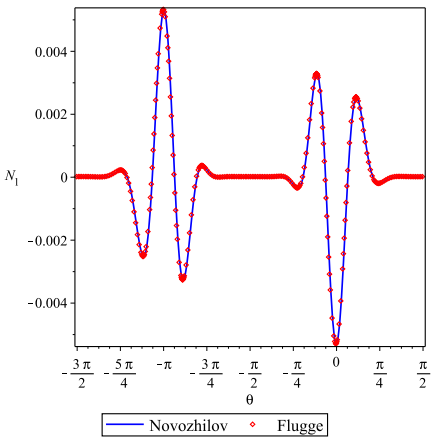

Figure 25: Shear force N_1 for problem as shown in Fig. 6. For this problem $P = Q_0$ (a) shear force N_1 from Novozhilon's formulation, which gives $N_1(0) = -0.5305164764e - 2[N/m]$ and $N_1(\pi) = 0.5305164764e - 2[N/m]$; (b) shear force N_1 from Hans Reissner's formulation, which gives $N_1(0) = -0.00530599792025551[N/m]$ and $N_1(\pi) = 0.005305164764e[N/m]$.

VIII. CONCLUSIONS AND FUTURE PERSPECTIVES

We have obtained an exact solution of the complex-form ODE for the symmetrical deformation of a torus. This solution is expressed by the Heun functions. However, as we stated, the Huen function cannot be split into real and imaginary parts explicitly. To solve this issue, we proposed a new strategy of transforming

Preprints (www.preprints.org) | NOT PEER-REVIEWED | Posted: 19 April 2021 doi:10.20944/preprints202012.0420.v3

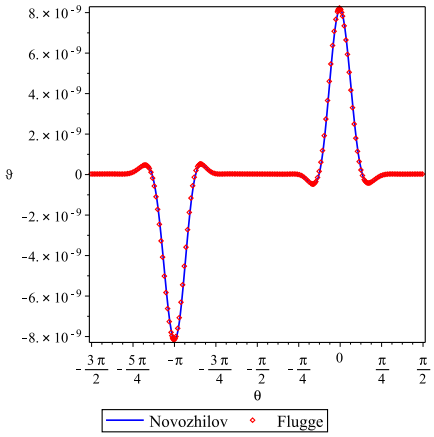

Figure 26: Problem as shown in Fig. 6. For this problem $P = 0$ (a) Rotation $\vartheta(\theta)$ from Novozhilon's formulation, which gives $\vartheta(0) = 8.17750337739746 \times 10^{-9}$ and $\vartheta(\pi) = -8.17750337739746 \times 10^{-9}$; (b) Rotation $\chi(\theta)$ from Hans Reissner's formulation, which gives $\chi(0) = 8.180964058$ and $\chi(\pi) = -8.180964058 \times 10^{-9}$.

the complex-form ODE of torus into an real-form ODE in terms of $A(\theta)$, $B(\theta)$, and $\triangle_z(\theta)$, which allowed us to easily deal with different kinds of boundary conditions.

To verify our formulation, we wrote a computational code in Maple and carried out some numerical simulations. The validation of our numerical results was confirmed and supported by both finite element analysis and Reissner's formulation. The numerical investigations show that the bending theory of shells should be used for torus deformation analysis due to its vary Gaussian curvature.

Regarding the future perspectives, it must be pointed out that the complex-form governing ODE of a torus is good for static deformation analysis but has some disadvantages, for instance, the the complex-form governing ODE cannot be used to deal with dynamical and buckling problems. This definitely limits the use of complex-form modeling. To overcome this shortcoming, displacement-type ODE of shells must be used (Sun 2010 [8]), which remains an open problem.

Acknowledgement:

The author is honored to have benefits from my supervisor Prof. Dr.Ing Wei Zhang (Wei Chang), who was the first Chinese scholar studied the deformation of torus, it is my privilege to dedicate this paper to the memories of Prof. W. Zhang for his great contribution to the analysis of elastic torus. The author appreciates my students: Mr. Guang-Kai Song, for providing finite element analysis data in Fig. 23, and preparation of Fig.2, Fig. 3 and 4; Mr. Xiang Li, for preparation of Fig.1 (a). I also wish to express my gratitude to anonymous reviewers for their high-level academic comments that helps me to enhance the quality of this paper.

Data availability: The data that support the findings of this study are available from the corresponding

author upon reasonable request.

[1] W. Chang (W. Zhang), Derspannungszustand in kreisringschale und ähnlichenSchalen mit Scheitelkreisringen unter drehsymmetrischer Belastung. Arbeitzur Erlangung des Grades eines Doctor-Ingenieurs der Technichen Hochschule, Berlin, 1944.(English translation: Zhang, W., Toroidal shells, Sci. Rep Nat. Tsinghua Univ., Ser A. 259-349 (1949))

[2] W.Z. Qian and S.C. Liang, Complex form equation and asymptotic solution. J. of Tsinghua University, 19(1979)(1) 27-47,

[3] Z.H. Xia and W. Zhang, The general solution for thin-walled curved tubes with arbitrary loadings and various boundary conditions. Int. J. Pressures and Piping 26(1986) 129-144.

[4] W. Zhang, W.M. Ren and B.H. Sun, Toroidal Shells - history, current situation and future. Fifth Conf. of Space Structures, Lanzhou, China 1990.

[5] R.J. Zhang and W. Zhang, Turning point solution for thin toroidal shell vibrations. Int. J. Solids Structures 27(1991)(10) 1311-1326.

[6] R.J. Zhang and W. Zhang, Toroidal shells under nonsymmetric loading. Int. J. Solids Structures, 31(1994) 2735-2750.

[7] B. Audoly and Y. Pomeau, Elasticity and Geometry. University of Cambridge, Cambridge, 2010

[8] B. Sun, Closed-form solution of axisymmetric slender elastic toroidal shells. J. of Engineering Mechanics, 136 (2010) 1281-1288.

[9] B. Sun, Toroidal Shells. (Nova Novinka, New York, 2012)

[10] R.A. Clark, R.A. and E. Reissner, Bending of curved tubes, Advances in Applied ;Hechanics. vol.II, Academic Press (1950)

[11] R.A. Clark, On the theory of thin elastic toroidal shells. J. Mech. Phys. Solids, 29(1950) 146-178.

[12] N.C. Dahl, Toroidal-shell expansion joints. J. of Applied Mechanics, ASME,20(1953) 497-503.

[13] V.V. Novozhilov, The Theory of Thin Shell. (Noordhoff, Groningen, 1959).

[14] S. Timoshenko and S. Woinowsky-Krieger, 1959. Theory of Plates and Shells. McGraw-Hill, New York.

[15] Flügge, W., 1973. Stresses in Shells. Springer-Verlag Berlin.

[16] Gol'denveizer, A.L., 1961. Theory of Elastic thin Shells. Pergamon Press, New York, 1961.

[17] B. Sun, Centenary studies of toroidal shells and in memory of Prof. Zhang Wei. Mechanics in Engineering, 37(2013). (In Chinese)

[18] Föppl, L., 1907. Vorlesungen Über Technische Mechanik. volume 5.B.G. Teubner, Leipzig, Germany.

[19] G. Weihs. Über Spannungs- und Formänderungszustände in dünnen. Hohlreifen. Halle a. S. 1911.

[20] H. Wissler, Festigkeiberechung von Ringsflachen. Promotionarbeit, Zurich (1916). https://doi.org/10.3929/ethz-a-000099037

[21] V.V. Kuznetsov and S.V. Levyakov, Nonlinear pure bending of toroidal shells of arbitrary cross-section. Int. J.

of Solids and Structures, 38(2001) 7343-7354.

[22] A. Zingoni, N. Enoma and N. Govender, Equatorial bending of an elliptic toroidal shell. Thin-Walled Structures, 96(2015) 286-294.

[23] W. Jiammeepreecha and S. Chucheepsakul, Nonlinear static analysis of an underwater elastic semi-toroidal shell. Thin-Walled Structures, 116(2017) 12-18.

[24] N. Enoma and A. Zingoni (2020). Analytical formulation and numerical modelling for multi-shell toroidal pressure vessels. Computers & Structures, 232(2020), Article 105811.

[25] H. Reissner, Spannungen in Kugelschalen (Kuppeln). Festschrift Heinrich Müller-Breslau (A. Kröner, Leipzig, 1912), 181-193

[26] E. Meissner,Über und Elastizitat Festigkeit dunner Schalen. Viertelschr. D. nature.Ges., Bd.60, Zurich (1915).

[27] F. Tölke, Ingenieur Archiv., 9 (1938), 282

[28] E. Reissner, On bending of curved thin-walled tubes. Proc. National Academy of Sci., (1949) 204-208.

[29] L.N. Tao, On toroidal shells. J. of Math. and Physics, 38,(1959) 130-134.

[30] C.R. Steele, Toroidal pressure vessels. J. Spacecr. Rocket., 2(1965) 937-943,

[31] B. Sun, Exact solution of Qian's equation of slender toroidal shells. Mechanics in Engineering, 38(2018)(5) 567-569.(in Chinese)

[32] A. Ronveaux, Heun's Differential Equations. Oxford University Press, 1995.

[33] https://en.wikipedia.org/wiki/Heun_function

[34] J.E. Marsden, L. Sirovich and S.S. Antman eds. Hypergeometric Functions and Their Applications. Texts in Applied Mathematics. 56. New York: Springer-Verlag, 1991.

[35] Marple https://www.maplesoft.com/